

AperTO - Archivio Istituzionale Open Access dell'Università di Torino

The angiostatic molecule Multimerin 2 is processed by MMP-9 to allow sprouting angiogenesis

This is the author's manuscript

Original Citation:

Availability:

This version is available <http://hdl.handle.net/2318/1660310> since 2021-04-19T12:14:25Z

Published version:

DOI:10.1016/j.matbio.2017.04.002

Terms of use:

Open Access

Anyone can freely access the full text of works made available as "Open Access". Works made available under a Creative Commons license can be used according to the terms and conditions of said license. Use of all other works requires consent of the right holder (author or publisher) if not exempted from copyright protection by the applicable law.

(Article begins on next page)

The angiostatic molecule Multimerin 2 is processed by MMP-9 to allow sprouting angiogenesis

Eva Andreuzzi^a, Roberta Colladel^a, Rosanna Pellicani^a, Giulia Tarticchio^a, Renato Cannizzaro^b, Paola Spessotto^a, Benedetta Bussolati^c, Alessia Brossa^c, Paolo De Paoli^d, Vincenzo Canzonieri^e, Renato V. Iozzo^f, Alfonso Colombatti^a, Maurizio Mongiat^a

a - Department of Translational Research, Experimental Oncology Division 2, CRO Aviano-IRCCS, National Cancer Institute, Aviano, Italy.

b - Division of Oncological Gastroenterology, CRO Aviano-IRCCS, National Cancer Institute, Aviano, Italy.

c - Department of Molecular Biotechnologies and Health Sciences, University of Turin, Italy.

d - Scientific Direction, CRO Aviano-IRCCS, National Cancer Institute, Aviano, Italy.

e - Pathology Unit, CRO Aviano-IRCCS, National Cancer Institute, Aviano, Italy.

f - Department of Pathology, Anatomy and Cell Biology and the Cancer Cell Biology and Signaling Program, Kimmel Cancer Center, Sidney Kimmel Medical College at Thomas Jefferson University, Philadelphia, PA 19107, USA

Correspondence to Maurizio Mongiat: Department of Translational Research, Experimental Oncology Division 2, CRO Aviano, via Franco Gallini 2, 33081 Aviano (PN) Italy. mmongiat@cro.it

ABSTACT

Angiogenesis is a crucial process occurring under physiological and pathological conditions, including cancer. The development of blood vessels is tightly regulated by a plethora of cytokines, endothelial cell (EC) receptors and extracellular matrix (ECM) components. In this context, we have shown that Multimerin 2 (MMRN2), an ECM molecule specifically secreted by ECs, exerts angiostatic functions by binding VEGFA and other pro-angiogenic cytokines. Here, we demonstrate that during angiogenic stimuli *MMRN2* mRNA levels significantly decrease. Furthermore, we provide evidence that MMRN2 is processed by matrix metalloproteinases (MMPs) including MMP-

9 and, to a lesser degree, by MMP-2. This proteolytic cleavage correlates with an increased migration of ECs. Accordingly, MMRN2 down-regulation is associated with an increased number of EC pseudopodia at the migrating front and this effect is attenuated using specific MMP-9 inhibitors. The down-modulation of MMRN2 occurs also in the context of tumor-associated angiogenesis. Immunofluorescence performed on tumor sections indicate a broad co-localization of MMP-9 and MMRN2, suggesting that the molecule may be extensively remodeled during tumor angiogenesis. Given the altered expression in tumors and the key role of MMRN2 in blood vessel function, we postulate that analyses of its expression may serve as a marker to predict the efficacy of the treatments. In conclusion, these data further support the role of MMRN2 as a key molecule regulating EC function and sprouting angiogenesis.

Introduction

Angiogenesis, the formation of new blood vessels from preexisting vessels, is a key process pertinent for reproduction, development, and wound repair [1,2]. The development of new vessels also plays a critical role in the onset and progress of many diseases, including cancer [3]. Pathological angiogenesis is a hallmark of cancer [4]. It is widely accepted that tumor growth is angiogenesis-dependent and blocking this process is regarded as a promising therapeutic approach to impair tumor growth [5,6]. Since the proposition of this groundbreaking hypothesis, many anti-angiogenic agents have been developed and are currently being utilized in the clinic. However, monotherapies with antiangiogenic drugs were not as effective as initially expected [7-12]. Fortunately, improvements have been achieved by combining anti-angiogenic treatments and standard chemotherapy with benefits in progression-free and overall survival [13,14]. Nevertheless, detrimental drawbacks of these approaches include resistance, reduced delivery of the drugs within tumors, and increased tumor hypoxia, which in turn may positively affect the development of metastasis [15,16]. Unfortunately, a significant fraction of patients does not receive benefit from the anti-angiogenic therapies and identification of clinical biomarkers is the focus of intense research [13,17-19].

The formation of blood vessels is tightly regulated and involves the coordinated interaction among a multitude of different cell types, cytokines, growth factors, and extracellular matrix (ECM) constituents [3,20-27]. ECM remodeling allows endothelial cell (EC) sprouting and is favored by activating several proteases. Matrix metalloproteinases (MMPs) [28] and in particular MMP-2, MMP-9, and MMP-14 play a key role in this context and are implicated in the local release of VEGF [29-31]. The MMPs encompass a large family of cation-dependent metallo-endo- or metallo-exo-peptidases responsible for coordinating a number of biological processes implicated in development and pathology [32-37].

Among the ECM molecules affecting angiogenesis, we have recently demonstrated that Multimerin 2 (MMRN2) halts angiogenic sprouting by sequestering VEGFA and impinging on the VEGF/VEGFR2 signaling axis [26,27]. MMRN2 belongs to the EDEN (EMI Domain ENdowed) protein family [38-40]. MMRN2 displays similar molecular architecture; although, unlike other

EDEN family members, its expression is confined in tight juxtaposition with the EC surface [41]. Given the strategic pan-endothelial localization of MMRN2, we hypothesized that, following an angiogenic stimulus, it could be degraded to allow efficient vessel sprouting. The results of this investigation demonstrate that MMRN2 cleavage favors EC motility and sprouting angiogenesis and further clarifies how this EC-specific molecule is regulated during angiogenesis.

Results

Down-regulation of MMRN2 expression promotes endothelial cell migration

Corroborating the angiostatic role of MMRN2, we depleted endogenous expression in HUVEC (Fig. 1A) with knockdown achieving a > 95% inhibition of the protein. The depletion of MMRN2 from HUVEC induced a significant increase of their motility in scratch test assays (Fig. 1B). Similar results were obtained in random motility assays where speed and distance covered by HUVEC were increased (Fig. 1C). Accordingly, the addition of recombinant MMRN2 (rMMRN2) reverted the effect (Fig. 1 C), further supporting the angiostatic role of MMRN2. We next analyzed the morphology of ECs in relation to MMRN2 expression by introducing a wound into the EC monolayer. Upon MMRN2 knockdown, ECs displayed a prominent motile phenotype with characteristic elongated shapes and an increased number of pseudopodia (Fig. 1D). In addition, MMRN2 expression was underrepresented at the EC migratory front and was particularly low along the pseudopodia (Fig. 1D,E). To verify if this phenomenon could be observed during vessel sprouting, we performed aortic ring assays. Importantly, MMRN2 expression was reduced in the tips of the sprouting vessels, whereas it was associated with that of CD31 in pre-existing vessels (Fig 1F).

MMRN2 is down-regulated and degraded in response to angiogenic stimuli

The above evidence, as well as our previous studies, suggest that MMRN2 is deposited in the late stages of vessel development and exerts a homeostatic role for ECs. Thus, it is possible that, once the angiogenic switch is activated, either MMRN2 expression is halted and/or the protein is degraded to allow efficient sprouting. To verify this hypothesis, we challenged HUVEC with

VEGFA, the major growth factor involved in angiogenesis. VEGFA significantly reduced *MMRN2* mRNA at 1 and 3 hours following treatment, with expression returning to near-normal levels at 6 hours (Fig. 2A). Similar results were obtained with FGF-2 (Fig. 2B). To verify if this could occur also in pathological angiogenesis, HUVEC were challenged with conditioned media (CM) from HT-29 cells. HUVEC displayed a significant down-regulation of *MMRN2* mRNA, which was decreased for up to 6 hours following VEGFA (Fig. 2C).

Accordingly, *MMRN2* protein levels decreased and remained low for a longer period compared to the mRNA (Fig. 2D). Utilizing the custom polyclonal antibody developed in our laboratory [27], we also analyzed the deposition of *MMRN2* by immunofluorescence over time and found that *MMRN2* formed an intricate fiber network in juxtaposition with the HUVEC monolayer. Interestingly, and in agreement with a homeostatic role for *MMRN2*, following the formation of a stable EC monolayer the protein levels increased over time (Fig. 2D,E). Further, treatment with VEGFA significantly impaired *MMRN2* deposition (Fig. 2E,F).

MMRN2 is degraded by MMP-9 upon angiogenic stimulation

The ability of EC to modify ECM constituents responding to signals received from the environment is critically important during angiogenesis and principally occurs through the activation of neutral proteinases, such as MMPs. Thus, concomitant to a transient reduction of its expression, we hypothesized that *MMRN2* degradation could allow efficient and protracted EC motility for robust vessel sprouting. To assess this hypothesis, HUVEC were challenged with VEGFA in the presence (or absence) of a generic MMP inhibitor (GM6001). The inhibitor abrogated the decrease of *MMNR2* prompted by VEGFA treatment (Fig. 3A). Since ECs primarily move through the ECM by MMP-2, MMP-9, and MT1-MMP [29,42-46] we queried and tested if *MMRN2* could be an MMP substrate. First, the expression of MMP-2 and MMP-9 increased following treatment with VEGFA and this correlated with decreased *MMRN2* expression (Fig 3A). Next, we used recombinant proteases and verified their activity on *MMRN2*. Unfortunately, we could not determine if MT1-MMP could cleave *MMRN2* as the protein was not soluble in the required digestion buffer (Supplementary Fig. S1A) and, unlike MMP-2 and MMP-9, the enzyme did not function in PBS

(Supplementary Fig. S1B). On the other hand, our analyses indicated that MMRN2 was processed by MMP-2 and MMP-9, producing at least a fragment of ~20 kDa (Fig 3B,C). Primarily, MMP-9 resulted in a significant reduction of full-length MMRN2, suggesting that it is more efficient in cleaving MMRN2 compared to MMP-2. These results were in accordance with the fact that there are more putative cleavage sites for MMP-9 than for MMP-2 within the primary MMRN2 amino acid sequence (Supplementary Fig. S1C). His-tagged MMRN2 recombinant protein produced by 293-EBNA cells was characterized by the presence of a ~ 20 kDa C-terminal His-tagged fragment recovered during purification. The production of this fragment was attenuated by the addition of a protease inhibitor cocktail and, interestingly, was not blocked by metalloproteinase inhibitors (data not shown). This observation suggests that besides ECs and MMPs, other cell types (and proteases) may target MMRN2 for degradation. Treatment of recombinant MMRN2 with MMP-9 induced formation of low molecular weight species in the N-terminal FLAG-tagged region and the His-tagged C-terminal region (Fig. 3D), confirming the presence of multiple MMP-9 cleavage sites at both termini. To verify the role of MMPs in controlling MMRN2 deposition/remodeling upon angiogenic stimuli, we treated HUVEC with VEGFA to stimulate MMPs in the presence or absence of MMP inhibitors. As shown (Fig. 3E,F), the use of a specific MMP-9 inhibitor prevented most of the MMP-driven MMRN2 degradation, whereas the contribution of MMP-2 in this process was subsidiary.

MMRN2 digestion by MMP-9 favors endothelial cell migration

To verify if MMRN2 degradation by MMP-9 is required for efficient EC migration, we performed a scratch assay in the presence of the MMP-9 inhibitor. HUVEC expressing basal levels of MMRN2 displayed a strong decrease in their migratory capability upon MMP-9 inhibition. Consistent with the aforementioned data (*cf.* Fig. 1B), RNAi-mediated silencing of MMRN2 alone was sufficient for increased HUVEC motility (Fig. 4A); in this case, however, the use of the MMP-9 inhibitor did not additively or synergistically impair their migration (Fig. 4A).

The immunofluorescence analysis performed on HUVEC under the same conditions indicated that the use of the specific MMP-9 inhibitor induced an increase of MMRN2 protein levels and a

concomitant reduction in the number of cell pseudopodia (Fig. 4B). On the contrary, the difference in the number of cell pseudopodia upon treatment with the MMP-9 inhibitor was not significant following MMRN2 depletion (Fig. 4B). These data are congruent with the non-additive and non-synergistic effect seen above (Fig. 4A).

Consistent results were obtained following treatment with recombinant MMP-9, which significantly increased EC motility in control cells but not following the down-regulation of MMRN2 expression (Fig. 5A,B). Interestingly, and unlike the effect exerted on EC migration, the processing of MMRN2 did not affect its potential to function as an adhesion substrate for ECs (Fig. 5C).

MMRN2 expression is down-regulated in tumor-associated endothelial cells

Next, we evaluated whether the expression of MMRN2 could be impaired in tumor associated vessels. The levels of *MMRN2* mRNA were lower in different tumor-derived ECs (PTEC, BTEC, ECK) when compared with the expression by HUVEC or HDMEC (Fig. 6A). Accordingly, multiple colorectal tumor biopsies exhibited decreased *MMRN2* expression compared to normal samples (Fig. 6B). In addition, immunofluorescence analyses performed on tumor biopsies revealed that MMP-9 staining was frequently near MMRN2 (Fig. 6C). Interestingly, altered and discontinuous MMRN2 staining was observed when MMP-9-positive cells were in close proximity with the vessels (Fig. 6D), suggesting extensive digestion during tumor-associated angiogenesis.

Taken together, these results indicate that expression of the angiostatic molecule MMRN2 is down-modulated during angiogenesis and digestion of MMRN2 promotes EC sprouting. These data further highlight the pivotal role of MMRN2 in regulating EC function during angiogenesis.

Discussion

In this study, for the first time, we sought to verify how the expression of the pan-endothelial cell molecule MMRN2 was regulated during angiogenesis in normal and pathological conditions. In our previous studies, we had demonstrated a homeostatic role for MMRN2 since its expression inhibited EC function by impinging on the VEGF/VEGFR2 signaling axis [26,27]. For this reason,

we hypothesized that in the presence of strong angiogenic signals, the expression of MMRN2 could be suppressed concomitant with protein degradation to allow efficient angiogenic sprouting.

In the present investigation, we have shown the angiostatic potential of MMRN2 in different experimental settings. We verified that increased EC migration following *MMRN2*-knockdown was attenuated by adding recombinant MMRN2, providing specificity for MMRN2 in this process. The use of an affinity purified polyclonal antibody produced in our laboratory allowed, for the first time, to detect endogenous protein synthesized by HUVEC. Strikingly, MMRN2 formed a fibrillar network juxtaposed to the cell surface. Silencing MMRN2 allowed an increase in the number of cell pseudopodia at the migratory front. These findings suggest that sole depletion of MMRN2 from the EC surface was sufficient to increase EC migration, which acquired a pronounced pro-migratory phenotype. Consistently, analyses of vessel sprouting from murine aortic rings revealed that the tips of the sprouting vessels were overall devoid of MMRN2, suggesting that expression of the molecule needed be halted and/or the protein degraded for efficient sprouting. Accordingly, treatment with VEGFA, as well as with FGF-2, significantly decreased *MMRN2* mRNA, with a return to baseline at late time points. This finding is intriguing since we have recently demonstrated that MMRN2 halts VEGFA activity [26,27]. Thus, it is possible that MMRN2/VEGFA may represent a feedback mechanism that acts to fully potentiate the pro-angiogenic effects of VEGFA, as was recently shown for pleiotrophin [47]. These results parallel Lee S. et al. showing that knockdown of CLEC14A, a type I transmembrane protein that binds MMRN2 [48], increases VEGFR2 signaling [49].

Interestingly, similar results were obtained following a tumor-derived stimulus. Treatment of HUVEC with conditioned media from tumor cells decreased *MMRN2* expression. This decrease was maintained for a significantly longer period of time when compared with the treatment with single cytokines. This may be likely due to the fact that HT-29 tumor cells secrete a plethora of pro-angiogenic factors [50] that are able to sustain the angiogenic signal over time.

While upon treatment with VEGFA, *MMRN2* mRNA decreased for over the course of a few hours, the protein levels remained lower for much longer, suggesting the existence of post-translational mechanisms (e.g. proteolysis) affecting protein stability following angiogenic stimuli.

Thus, we analyzed the activity of matrix metalloproteases MT1-MMP, MMP-2, and MMP-9, which are the major pro-angiogenic MMPs. Notably, MMP-2 and MMP-9 are required for the angiogenic switch during tumorigenesis [29,46,51]. MMRN2 was cleaved by MMP-9 and, less efficiently, by MMP-2. Inhibiting MMP-9 abrogated cell migration in EC expressing normal levels of MMRN2, implying that MMRN2 degradation represents a crucial event for EC motility and, more broadly, angiogenesis. The activity of MMP-2 and MMP-9 on MMRN2 does not alter the capability of EC to adhere to cleaved MMRN2 suggesting that, following digestion, ECs may ultimately use MMRN2 as a substrate to move and invade the surrounding tissue during neo-angiogenesis.

Degradation of the vascular basement membrane and ECM remodeling is required for EC migration and invasion into the surrounding tissue. The processing of MMRN2 by MMPs further supports the notion of a homeostatic and pro-angiostatic role for this molecule. In addition, since MMRN2 sequesters VEGFA and other angiogenic-active cytokines [26,27], it is possible that digestion of MMRN2 may induce the release of these factors. This mechanism may represent a further, indirect method, by which MMRN2 degradation leads to improved angiogenic sprouting.

The expression of MMRN2 is altered in several tumor types [52-55] and this unravels different scenarios from a therapeutic perspective. First, MMRN2 expression may vary between individuals. Second, our results demonstrate that *MMRN2* mRNA is low in tumor-associated ECs and tumor vessels. Moreover, immunofluorescent analyses performed on human colorectal cancer samples showed numerous MMP-9-positive cells adjacent to MMRN2. This tight juxtaposition was often associated with MMRN2 staining suggestive of ongoing degradation. Thus, given the role of MMRN2 in VEGFA regulation, bioavailability, and blood vessel formation in conjunction with its altered expression in tumors, the analysis of MMRN2 expression may represent an important prognosticator to predict the efficacy of costly antiangiogenic therapies.

Conversely, impaired expression of MMRN2 in tumor-associated vessels may influence efficiency of the vasculature and, in turn, therapeutic efficacy. Additional investigations are currently ongoing to better clarify the role of MMRN2 in this context.

Taken together, these results provide further evidence that identify MMRN2 as a key molecule in regulating EC function and demonstrates that, during the angiogenic stimulation, its expression is controlled both transcriptionally and post-translationally for efficient EC sprouting.

Experimental procedures

Cells and reagents

Human Dermal Microvascular Endothelial Cells (HDMEC) were from (ScienCell Research Laboratories, Inc., San Diego, CA, USA). Human Umbilical Vein Endothelial Cells (HUVEC) were isolated from the human umbilical cord vein as previously described [27]. Both cells were cultured in endothelial cell medium (ScienCell Research Laboratories, Inc., San Diego, CA, USA). The human colorectal adenocarcinoma (HT-29) cell line was obtained from American Type Culture Collection (ATCC, Manassas, VA, USA) and cultured in Dulbecco's Modified Eagle Medium (DMEM) containing 10% FBS and 1% penicillin-streptomycin. Embryonic kidney 293-EBNA (Epstein-Barr Nuclear Antigen) cells were a gift from Rupert Timpl (Max Planck, Munich, Germany) and cultured in DMEM (Sigma-Aldrich, Milan, Italy) containing 10% FBS, 1% Penicillin-Streptomycin and 250 µg/ml of G418 (Sigma-Aldrich, Milan, Italy); 0.5 µg/ml of puromycin (Sigma-Aldrich, Milan, Italy) were added after transfection. All cells were maintained at 37°C in a humidified 5% CO₂ atmosphere.

The anti-His antibody was from Abgent (San Diego, CA, USA), the Ni-NTA agarose was from QIAGEN (Milan, Italy). The anti-MMRN2 polyclonal antibody was obtained upon immunization of a rabbit with 150 µg of a recombinant MMRN2 fragment corresponding to the N-terminal gC1q domain. The antibody was affinity purified from the rabbit serum by means of the CNBr-activated Sepharose 4B resin (Amersham, GE-Healthcare, Milan, Italy). Secondary horse radish peroxidase (HRP)-conjugated antibodies were from Amersham (GE-Healthcare, Milan, Italy). The anti-mouse-CD31 antibody was from BD Biosciences and the anti MMP-9 from Millipore (Merck-Millipore, Milan, Italy). The secondary antibodies conjugated with Alexa Fluor 488, 568 and TO-PRO[®] 3 were from Invitrogen (Milan, Italy). Secondary HRP-conjugated antibodies were from Amersham (Milan,

Italy). Recombinant human VEGF-A₁₆₅ was from R&D systems Inc. (MN,USA). Collagen R was from Serva Electrophoresis (Aurogene, Rome, Italy). Recombinant MMP-2, MMP-9 and Mt-MMP1 were from Giotto Biotech (Firenze, Italy). The generic matrix metalloproteinases inhibitor (GM6001), and the specific MMP-9 and MMP-2 inhibitors (MMP-9 inhibitor I and MMP-2 inhibitor I) were from Calbiochem (Merck-Millipore, Milan, Italy). Recombinant fibronectin was from Sigma-Aldrich (Milan, Italy).

Preparation of cell lysates and Western blot analysis

For MMRN2 expression studies, HUVEC were treated with VEGFA (30 ng/ml) with or without the protease inhibitor GM6001 (20 μ M) for different time points. The cells were then lysed in cold buffer (1 mM CaCl₂, 1 mM MgCl₂, 15 mM Tris-HCl pH 7.2, 150 mM NaCl, 1% TrytonX100, 0.1% SDS, 0.1% Na Deoxycholate) containing 25 mM NaF, 1 mM DTT, 1 mM Na₃VO₄ and the protease inhibitors cocktail (Roche, Monza, Italy). For Western blot analyses, proteins were resolved in 4-20% Criterion Precast Gels (Bio-Rad, Hercules, CA, USA) and transferred onto Hybond-ECL nitrocellulose membranes (Amersham, MI, Italy). Membranes were blocked with 5% BSA in TBS-T (100 mM Tris-HCl pH 7.5, 0.9% NaCl, 0.1% Tween 20) and probed with the appropriate antibodies. The blots were finally developed using ECL (Western blotting detection, Amersham Biosciences, MI, Italy) and exposed to X-ray films or acquired using the ChemiDoc Touch Imaging System (Bio-Rad, Hercules, CA, USA). Alternatively, the Odyssey infrared imaging system was used (Li-COR Biosciences, Lincoln, NE, USA).

Cell transfection, expression and purification of recombinant proteins

293-EBNA cells were transfected by electroporation with different pCEP-Pu constructs and selected in the presence of 0.5 μ g/ml of puromycin and 250 μ g/ml of G418. Positive clones were isolated and the expression analyzed by Western blotting. Confluent 293-EBNA cells were then incubated in serum-free medium for 48 hours, the media were collected and equilibrated with a buffer containing 50 mM NaH₂PO₄, 150 mM NaCl, 10 mM imidazole. The proteins were purified by means of the Ni-NTA resin and eluted with the elution buffer (50 mM NaH₂PO₄, 300 mM NaCl, 250

mM imidazole). The different fractions were analyzed by SDS-PAGE followed by Coomassie blue staining. Protein fractions were then dialyzed against PBS and concentrated using polyethylene glycol (PEG).

Recombinant adenovirus

For the down-regulation of the expression of endogenous MMRN2 an adenoviral construct was created [27] carrying the following siRNA sequence: siRNA 4: 5'-GCAGACAGTGAAGTTCAACACCACATACA-3'. 2×10^5 HUVEC were transduced using the siRNA control or siMMRN2 constructs using 500 multiplicity of infection (MOI).

Random motility and scratch assays

For the random motility assays, 3×10^3 HUVEC transduced with control or MMRN2 adenoviral constructs, were seeded on 48 well plates and allowed to adhere to the culture plate. Cells were then starved for 5 hours in ECM-basal medium containing 20% ECM complete medium. Cells were treated with PBS or recombinant MMRN2 (5 μ g/ml) or with recombinant MMP-9 (25 ng/ml). Cell movement was monitored over time with the AF6000 Time-lapse Imaging System (Leica, Wetzlar, Germany). Cell Distance and speed were calculated with the dedicated software. For the scratch test analyses, HUVECs were seeded in a 24-multiwell dish and allowed to grow until they reached confluency. Confluent cells were starved overnight with ECM-basal medium with 5% FBS. A scratch wound was made using a sterile pipette tip, cells were then washed and incubated with medium containing 2% serum in the presence of DMSO or protease inhibitors (20 μ M of the generic metalloproteinase inhibitor GM6001, 25 μ M of the MMP-9 inhibitor and 20 μ M of the MMP-2 inhibitor). Time course analysis was carried out by LEICA Time-lapse Imaging System (LEICA, Wetzlar, Germany). For the immunofluorescence analyses HUVEC cells were seeded on glass cover slides. The scratch wound was made and 6 hours later the cells were fixed with 4% (w/v) paraformaldehyde. The number of migrating cells and the number of pseudopodia per cell were evaluated by counting.

Real-Time PCR analyses

For the MMRN2 expression studies in HUVEC, 10^5 cells were seeded on 12 well plates and after a 3 hour serum starvation in ECM-basal medium, cells were treated with VEGFA (30 ng/ml), FGF-2 (30 ng/ml) or PBS for the indicated time points. Alternatively, cells were treated with the conditioned medium from HT-29 cells or with control medium. Breast, prostate and kidney tumor endothelial cells (BTEC, PTEC and KTEC, respectively) were isolated as previously described [56-58] and grown to confluency for RNA extraction. RNA was extracted with the Trizol reagent (Invitrogen, Milan, Italy). Reverse transcription was performed using AMV-RT and exanucleotides (Promega, Milan, Italy). Real-time PCR were carried out using the iQ™ SYBR® Green Supermix (Bio-Rad, Hercules, CA, USA) using the following oligonucleotides: GAPDH 5'-GAGAGACCCTCACTGCTG-3', 5'-GATGGTACATGACAAGGTGC-3'; MMRN2 5'-AGGCTTCCAGTACTAGCCTCTCT -3', 5'-GGTAGGGGCACCAGTTACG-3'; CD31 5'-AACAGTGTTGACATGAAGAGCC-3', 5'-TGTA AACAGCAGCAGTCATCCTT-3'. The primer efficiency was ~100%, thus the comparative Ct method ($2^{-\Delta\Delta Ct}$) was applied for the analyses. RNA was extracted from tumor frozen sections with the Trizol reagent and processed as described above.

In vitro protein digestion assays

For the digestion assays 2 μ g of recombinant MMRN2 or fibronectin were placed in digestion buffer (50 mM Tris HCl pH 7.5, 150 mM NaCl, 10 mM CaCl_2) or PBS in the presence or not of the recombinant proteases in a ratio protease:protein of 1:10 and placed at 37°C for 16 hours. Protein digestion was verified by SDS-PAGE followed by Coomassie blue staining. Alternatively, the analysis was conducted by Western blot using the anti-FLAG antibody to detect the N-terminal fragments and the anti-His antibody to detect the C-terminal fragments.

Cell adhesion assays

For the adhesion assays the wells of ELISA plates were coated overnight at 4°C with 500 ng of collagen type I (used as a positive control) or 500 ng of MMRN2 treated or not with 50ng of

recombinant MMP-9 for 16 hours as described above. MMRN2 and MMP-9 were incubated as above and coated on ELISA plates and served as positive or negative control, respectively. After saturation with 1% BSA, HUVEC cells were then seeded at 20×10^4 cells/well in FBS-free medium. After 30 minutes of adhesion, floating cells were removed by washing and the adhered cells stained with crystal violet and counted.

Immunofluorescence analyses

HUVEC were seeded on cover glass slides placed in a 24 well plate and permitted to adhere. After 2 hours, the culture medium was replaced by ECM-basal medium with 0.5% FBS and the cells were treated with VEGFA (30 ng/ml) or PBS for 3, 6, 12 and 24 hours at 37°C. Next, cells were fixed with 4% (w/v) paraformaldehyde for 15 minutes at room temperature. For the experiments involving the use of metalloproteinase inhibitors, HUVEC cells were let growth for two days on cover glass slides and then treated with VEGF-A (30 ng/ml) or PBS in the presence of a concentration of 20 and 25 μ M of the MMP-2 and MMP-9 inhibitors, respectively. DMSO was used as control. After 3 and 6 hours, cells were fixed as above. The cells were saturated with blocking buffer (PBS-2% BSA) for 1 hour and incubated overnight at 4°C with the α -MMRN2 antibody. Next, the actin cytoskeleton was stained with phalloidin for 1 hour at room temperature. Slides were finally mounted in Mowiol containing 2.5% (w/v) of 1,4-diazabicyclo-(2,2,2)-octane (DABCO). Images were acquired with a Leica TCS SP8 Confocal system (Leica Microsystems Heidelberg, Mannheim, Germany), using the Leica Confocal Software (LCS). Fluorescence intensity and quantification was evaluated by means of the Volocity software (PerkinElmer Inc., Waltham, MA, USA).

Immunofluorescence analysis of tumor samples

Three- μ m sections were obtained from paraffin-embedded colorectal cancer samples. Deparaffinized section were placed in the microwave for 20 min at 650 watt in 0,01M citrate buffer at pH=6. Air dried samples hydrated in PBS for 15 min, placed in 1% Triton-X100 for 3 min, blocked in 10% normal goat serum for 1 hour at RT and stained over night at 4°C with anti-MMP-9

and anti-MMRN2 antibodies. The specific Alexa Fluor secondary antibodies were applied for 1 h at room temperature with TO-PRO[®] 3 (ThermoFisher Scientific, Waltham, MA, USA) for nuclei visualization. Finally, slides were mounted and analyzed as described above.

Aortic ring assays

The aortic ring assays were performed as previously described [59]. Six week old male C57BL/6 mice were used for aortic isolation. After dissection, fat tissue was removed and thoracic aortas were sectioned at 1 mm intervals and embedded in 1 mg/ml of collagen R. The rings were cultured in Opti-MEM (Gibco, ThermoFisher Scientific, Waltham, MA, USA) with 30 ng/ml of VEGFA for 10 days. The collagen gels were fixed in 4% PFA for 20 minutes, treated for 15 min at room temperature with PBS containing 0.25% TritonX-100 and saturated with blocking buffer (PBS-1% BSA) for 90 min. The gels were then incubated overnight at 4°C with the anti-MMRN2 and anti-CD31 antibodies diluted in PBlec buffer (PBS, pH 6.8 with 1 mM CaCl₂, 0.1 mM MgCl₂, 0.1 mM MnCl₂, 1% Tween-20). After a 1 hour incubation at room temperature with the appropriate secondary fluorescent antibodies and TO-PRO[®] 3 for nuclei, the gels were gently detached from the plastic well and mounted on glass slides with Mowiol containing 2,5% (w/v) of 1,4-diazabicyclo-(2,2,2)-octane (DABCO). Images were acquired with a Leica TCS SP2 confocal system (Leica Microsystems Heidelberg, Mannheim, Germany), using the Leica Confocal Software (LCS).

Statistical analysis

Statistical analyses were performed with the GraphPad Prism 6 software (Graphpad) and the values represent the mean \pm standard deviation obtained with not less than three measurements on randomized samples. Since the variance between groups was similar and values were normally distributed, the statistical significance of the differences was determined by the Student t test for the comparisons between two groups; for more than two groups, the 1-way ANOVA analysis of variance was used, according to the Bonferroni method. For all evaluations reported, the investigators were blinded to treatment of subjects and to analyses. Differences were considered statistically significant when $P \leq 0.05$.

Author contribution: Eva Andreuzzi: performed most of the experiments, prepared figures and critically discussed the results and manuscript; Roberta Colladel: performed the initial experiments on MMRN2 digestion; Rosanna Pellicani: performed the adenoviral transfections; Giulia Tarticchio: performed the Real-Time PCR analyses and the MMP-9 staining; Renato Cannizzaro: collected the colorectal cancer biopsies; Paola Spessotto: helped with the sample collection; Benedetta Bussolati and Alessia Brossa performed the analyses using tumor-derived ECs; Paolo De Paoli: partially supported the personnel involved in the study; Vincenzo Canzonieri: provided the samples for the MMP-9 analyses; Renato V. Iozzo and Alfonso Colombatti: critically reviewed the manuscript; Maurizio Mongiat conceived the study and wrote the manuscript.

Conflict of interest: The authors declare that they have no conflict of interest.

Acknowledgments

We thank Monica Schiappacassi for help with the adenoviral and lentiviral constructs, and Gustavo Baldassarre for constructive discussion. We also thank the Associazione Italiana per la Ricerca sul Cancro (AIRC, grant # IG-2012-12718 to M. Mongiat) and the Italian Ministry of Health (grant # RF-2010-2312580 to M. Mongiat).

Received 16 March 2017

Received in revised form 18 April 2017

Accepted 20 April 2017

Appendix A:

Supplementary data

Keywords:

angiogenesis,
endothelial cells,

tumor microenvironment.

Abbreviations used:

Multimerin 2 (MMRN2), endothelial cell (EC), extracellular matrix (ECM), fibroblast growth factor 2 (FGF-2), vascular endothelial growth factor A (VEGFA), vascular endothelial growth factor receptor 2 (VEGFR2), matrix metalloproteinase (MMP), multiplicity of infection (MOI).

References

- [1] Risau W. Mechanisms of angiogenesis. *Nature*. 1997; 386: 671-674.
- [2] Carmeliet P. Mechanisms of angiogenesis and arteriogenesis. *Nat Med*. 2000; 6: 389-395.
- [3] Carmeliet P. Angiogenesis in health and disease. *Nat Med*. 2003; 9: 653-660.
- [4] Hanahan D, Weinberg RA. Hallmarks of cancer: the next generation. *Cell*. 2011; 144: 646-674.
- [5] Folkman J. Tumor angiogenesis: therapeutic implications. *N Engl J Med*. 1971; 285: 1182-1186.
- [6] Folkman J. Angiogenesis. *Annu Rev Med*. 2006; 57: 1-18.
- [7] Carmeliet P, Jain RK. Molecular mechanisms and clinical applications of angiogenesis. *Nature*. 2011; 473: 298-307.
- [8] Cascone T, Heymach JV. Targeting the angiopoietin/Tie2 pathway: cutting tumor vessels with a double-edged sword? *J Clin Oncol*. 2012; 30: 441-444.
- [9] Chung AS, Lee J, and Ferrara N. Targeting the tumour vasculature: insights from physiological angiogenesis. *Nat Rev Cancer*. 2010; 10: 505-514.
- [10] Ohtsu A, Shah MA, Van CE, Rha SY, Sawaki A, Park SR, Lim HY, Yamada Y, Wu J, Langer B, Starnawski M, and Kang YK. Bevacizumab in combination with chemotherapy as first-line therapy in advanced gastric cancer: a randomized, double-blind, placebo-controlled phase III study. *J Clin Oncol*. 2011; 29: 3968-3976.
- [11] Okines A, Cunningham D. Current perspective: bevacizumab in colorectal cancer--a time for reappraisal? *Eur J Cancer*. 2009; 45: 2452-2461.
- [12] Ferrara N. VEGF as a therapeutic target in cancer. *Oncology*. 2005; 69 Suppl 3: 11-16.
- [13] Hurwitz H, Fehrenbacher L, Novotny W, Cartwright T, Hainsworth J, Heim W, Berlin J, Baron A, Griffing S, Holmgren E, Ferrara N, Fyfe G, Rogers B, Ross R, and Kabbinavar F. Bevacizumab plus irinotecan, fluorouracil, and leucovorin for metastatic colorectal cancer. *N Engl J Med*. 2004; 350: 2335-2342.

- [14] Cunningham D, Starling N, Rao S, Iveson T, Nicolson M, Coxon F, Middleton G, Daniel F, Oates J, and Norman AR. Capecitabine and oxaliplatin for advanced esophagogastric cancer. *N Engl J Med.* 2008; 358: 36-46.
- [15] Ebos JM, Lee CR, Cruz-Munoz W, Bjarnason GA, Christensen JG, and Kerbel RS. Accelerated metastasis after short-term treatment with a potent inhibitor of tumor angiogenesis. *Cancer Cell.* 2009; 15: 232-239.
- [16] Paez-Ribes M, Allen E, Hudock J, Takeda T, Okuyama H, Vinals F, Inoue M, Bergers G, Hanahan D, and Casanovas O. Antiangiogenic therapy elicits malignant progression of tumors to increased local invasion and distant metastasis. *Cancer Cell.* 2009; 15: 220-231.
- [17] Van CE, Tabernero J, Lakomy R, Prenen H, Prausova J, Macarulla T, Ruff P, van Hazel GA, Moiseyenko V, Ferry D, McKendrick J, Polikoff J, Tellier A, Castan R, and Allegra C. Addition of aflibercept to fluorouracil, leucovorin, and irinotecan improves survival in a phase III randomized trial in patients with metastatic colorectal cancer previously treated with an oxaliplatin-based regimen. *J Clin Oncol.* 2012; 30: 3499-3506.
- [18] Grothey A, Van CE, Sobrero A, Siena S, Falcone A, Ychou M, Humblet Y, Bouche O, Mineur L, Barone C, Adenis A, Tabernero J, Yoshino T, Lenz HJ, Goldberg RM, Sargent DJ, Cihon F, Cupit L, Wagner A, and Laurent D. Regorafenib monotherapy for previously treated metastatic colorectal cancer (CORRECT): an international, multicentre, randomised, placebo-controlled, phase 3 trial. *Lancet.* 2013; 381: 303-312.
- [19] Garcia-Carbonero R, Rivera F, Maurel J, Ayoub JP, Moore MJ, Cervantes A, Asmis TR, Schwartz JD, Nasroulah F, Ballal S, and Tabernero J. An open-label phase II study evaluating the safety and efficacy of ramucirumab combined with mFOLFOX-6 as first-line therapy for metastatic colorectal cancer. *Oncologist.* 2014; 19: 350-351.
- [20] Mongiat M, Marastoni S, Ligresti G, Lorenzon E, Schiappacassi M, Perris R, Frustaci S, and Colombatti A. The extracellular matrix glycoprotein elastin microfibril interface located protein 2: a dual role in the tumor microenvironment. *Neoplasia.* 2010; 12: 294-304.

- [21] Adams JC, Lawler J. The thrombospondins. *Cold Spring Harb Perspect Biol.* 2011; 3: a009712.
- [22] Mongiat M, Andreuzzi E, Tarticchio G, and Paulitti A. Extracellular Matrix, a Hard Player in Angiogenesis. *Int J Mol Sci.* 2016; 17.
- [23] Torres A, Gubbiotti MA, and Iozzo RV. Decorin-inducible Peg3 Evokes Beclin 1-mediated Autophagy and Thrombospondin 1-mediated Angiostasis. *J Biol Chem.* 2017.
- [24] Pozzi A, Yurchenco PD, and Iozzo RV. The nature and biology of basement membranes. *Matrix Biol.* 2017; 57-58: 1-11.
- [25] Gubbiotti MA, Neill T, and Iozzo RV. A current view of perlecan in physiology and pathology: A mosaic of functions. *Matrix Biol.* 2017; 57-58: 285-298.
- [26] Colladel R, Pellicani R, Andreuzzi E, Paulitti A, Tarticchio G, Todaro F, Colombatti A, and Mongiat M. MULTIMERIN2 binds VEGF-A primarily via the carbohydrate chains exerting an angiostatic function and impairing tumor growth. *Oncotarget.* 2016; 7: 2022-2037.
- [27] Lorenzon E, Colladel R, Andreuzzi E, Marastoni S, Todaro F, Schiappacassi M, Ligresti G, Colombatti A, and Mongiat M. MULTIMERIN2 impairs tumor angiogenesis and growth by interfering with VEGF-A/VEGFR2 pathway. *Oncogene.* 2012; 31: 3136-3147.
- [28] Apte SS, Parks WC. Metalloproteinases: A parade of functions in matrix biology and an outlook for the future. *Matrix Biol.* 2015; 44-46: 1-6.
- [29] Fang J, Shing Y, Wiederschain D, Yan L, Butterfield C, Jackson G, Harper J, Tamvakopoulos G, and Moses MA. Matrix metalloproteinase-2 is required for the switch to the angiogenic phenotype in a tumor model. *Proc Natl Acad Sci U S A.* 2000; 97: 3884-3889.
- [30] Belotti D, Paganoni P, Manenti L, Garofalo A, Marchini S, Taraboletti G, and Giavazzi R. Matrix metalloproteinases (MMP9 and MMP2) induce the release of vascular endothelial growth factor (VEGF) by ovarian carcinoma cells: implications for ascites formation. *Cancer Res.* 2003; 63: 5224-5229.

- [31] Deryugina EI, Quigley JP. Pleiotropic roles of matrix metalloproteinases in tumor angiogenesis: contrasting, overlapping and compensatory functions. *Biochim Biophys Acta*. 2010; 1803: 103-120.
- [32] Arpino V, Brock M, and Gill SE. The role of TIMPs in regulation of extracellular matrix proteolysis. *Matrix Biol*. 2015; 44-46: 247-254.
- [33] Wells JM, Gaggari A, and Blalock JE. MMP generated matrikines. *Matrix Biol*. 2015; 44-46: 122-129.
- [34] Deryugina EI, Quigley JP. Tumor angiogenesis: MMP-mediated induction of intravasation- and metastasis-sustaining neovasculature. *Matrix Biol*. 2015; 44-46: 94-112.
- [35] Rohani MG, Parks WC. Matrix remodeling by MMPs during wound repair. *Matrix Biol*. 2015; 44-46: 113-121.
- [36] Duarte S, Baber J, Fujii T, and Coito AJ. Matrix metalloproteinases in liver injury, repair and fibrosis. *Matrix Biol*. 2015; 44-46: 147-156.
- [37] Eckhard U, Huesgen PF, Schilling O, Bellac CL, Butler GS, Cox JH, Dufour A, Goebeler V, Kappelhoff R, Keller UA, Klein T, Lange PF, Marino G, Morrison CJ, Prudova A, Rodriguez D, Starr AE, Wang Y, and Overall CM. Active site specificity profiling of the matrix metalloproteinase family: Proteomic identification of 4300 cleavage sites by nine MMPs explored with structural and synthetic peptide cleavage analyses. *Matrix Biol*. 2016; 49: 37-60.
- [38] Braghetta P, Ferrari A, De GP, Zanetti M, Volpin D, Bonaldo P, and Bressan GM. Overlapping, complementary and site-specific expression pattern of genes of the EMILIN/Multimerin family. *Matrix Biol*. 2004; 22: 549-556.
- [39] Colombatti A, Spessotto P, Doliana R, Mongiat M, Bressan GM, and Esposito G. The EMILIN/Multimerin family. *Front Immunol*. 2011; 2: 93.
- [40] Doliana R, Canton A, Bucciotti F, Mongiat M, Bonaldo P, and Colombatti A. Structure, chromosomal localization, and promoter analysis of the human elastin microfibril interfase located protein (EMILIN) gene. *J Biol Chem*. 2000; 275: 785-792.

- [41] Christian S, Ahorn H, Novatchkova M, Garin-Chesa P, Park JE, Weber G, Eisenhaber F, Rettig WJ, and Lenter MC. Molecular cloning and characterization of EndoGlyx-1, an EMILIN-like multisubunit glycoprotein of vascular endothelium. *J Biol Chem*. 2001; 276: 48588-48595.
- [42] Moses MA. The regulation of neovascularization of matrix metalloproteinases and their inhibitors. *Stem Cells*. 1997; 15: 180-189.
- [43] Egeblad M, Werb Z. New functions for the matrix metalloproteinases in cancer progression. *Nat Rev Cancer*. 2002; 2: 161-174.
- [44] van Hinsbergh VW, Engelse MA, and Quax PH. Pericellular proteases in angiogenesis and vasculogenesis. *Arterioscler Thromb Vasc Biol*. 2006; 26: 716-728.
- [45] Handsley MM, Edwards DR. Metalloproteinases and their inhibitors in tumor angiogenesis. *Int J Cancer*. 2005; 115: 849-860.
- [46] Bergers G, Brekken R, McMahon G, Vu TH, Itoh T, Tamaki K, Tanzawa K, Thorpe P, Itohara S, Werb Z, and Hanahan D. Matrix metalloproteinase-9 triggers the angiogenic switch during carcinogenesis. *Nat Cell Biol*. 2000; 2: 737-744.
- [47] Poimenidi E, Theodoropoulou C, Koutsoumpa M, Skondra L, Droggiti E, van den Broek M, Koolwijk P, and Papadimitriou E. Vascular endothelial growth factor A (VEGF-A) decreases expression and secretion of pleiotrophin in a VEGF receptor-independent manner. *Vascul Pharmacol*. 2016; 80: 11-19.
- [48] Noy PJ, Lodhia P, Khan K, Zhuang X, Ward DG, Verissimo AR, Bacon A, and Bicknell R. Blocking CLEC14A-MMRN2 binding inhibits sprouting angiogenesis and tumour growth. *Oncogene*. 2015; 34: 5821-5831.
- [49] Lee S, Rho SS, Park H, Park JA, Kim J, Lee IK, Koh GY, Mochizuki N, Kim YM, and Kwon YG. Carbohydrate-binding protein CLEC14A regulates VEGFR-2- and VEGFR-3-dependent signals during angiogenesis and lymphangiogenesis. *J Clin Invest*. 2017; 127: 457-471.

- [50] Chung S, Dwabe S, Elshimali Y, Sukhija H, Aroh C, and Vadgama JV. Identification of Novel Biomarkers for Metastatic Colorectal Cancer Using Angiogenesis-Antibody Array and Intracellular Signaling Array. *PLoS ONE*. 2015; 10: e0134948.
- [51] Rundhaug JE. Matrix metalloproteinases and angiogenesis. *J Cell Mol Med*. 2005; 9: 267-285.
- [52] Shield-Artin KL, Bailey MJ, Oliva K, Liovic AK, Barker G, Dellios NL, Reisman S, Ayhan M, and Rice GE. Identification of ovarian cancer-associated proteins in symptomatic women: a novel method for semi-quantitative plasma proteomics. *Proteomics Clin Appl*. 2012n/a.
- [53] Soltermann A, Ossola R, Kilgus-Hawelski S, von EA, Suter T, Aebersold R, and Moch H. N-glycoprotein profiling of lung adenocarcinoma pleural effusions by shotgun proteomics. *Cancer*. 2008; 114: 124-133.
- [54] Zanivan S, Maione F, Hein MY, Hernandez-Fernaund JR, Ostasiewicz P, Giraudo E, and Mann M. SILAC-Based Proteomics of Human Primary Endothelial Cell Morphogenesis Unveils Tumor Angiogenic Markers. *Mol Cell Proteomics*. 2013; 12: 3599-3611.
- [55] Huber MA, Kraut N, Schweifer N, Dolznig H, Peter RU, Schubert RD, Scharffetter-Kochanek K, Pehamberger H, and Garin-Chesa P. Expression of stromal cell markers in distinct compartments of human skin cancers. *J Cutan Pathol*. 2006; 33: 145-155.
- [56] Grange C, Bussolati B, Bruno S, Fonsato V, Sapino A, and Camussi G. Isolation and characterization of human breast tumor-derived endothelial cells. *Oncol Rep*. 2006; 15: 381-386.
- [57] Fiorio PA, Brossa A, Bernardini M, Genova T, Grolez G, Villers A, Leroy X, Prevarskaya N, Gkika D, and Bussolati B. Differential sensitivity of prostate tumor derived endothelial cells to sorafenib and sunitinib. *BMC Cancer*. 2014; 14: 939.
- [58] Bussolati B, Deambrosis I, Russo S, Deregibus MC, and Camussi G. Altered angiogenesis and survival in human tumor-derived endothelial cells. *FASEB J*. 2003; 17: 1159-1161.
- [59] Aplin AC, Fogel E, Zorzi P, and Nicosia RF. The aortic ring model of angiogenesis. *Methods Enzymol*. 2008; 443: 119-136.

Figure legends.

Fig. 1. Depletion of MMRN2 leads to increased EC pseudopodia and migration. (A). Western blot of MMRN2 expression in HUVEC following transduction with control (siScr) or MMRN2 specific (siMMRN2) siRNA adenoviral constructs. β -Actin was used for normalization. (B). Representative images of scratch tests following depletion of MMRN2 and evaluation of migration (%) and distance (μm) covered by ECs after 6 hours post-scratch. Scale bar = 160 μm . Statistics were obtained using the paired Student's t-test. (C) Graphs representing random motility of HUVEC cells transduced with the control (siScr) or MMRN2 specific (siMMRN2) adenoviral constructs in the presence of recombinant MMRN2 (rMMRN2); and evaluation of the total and euclid distance and speed of ECs. Statistics were obtained via one-way ANOVA. (D) Representative images of HUVEC transduced with control (siScr) or MMRN2 specific (siMMRN2) adenoviral constructs following scratch. Cells were stained with anti-MMRN2 antibody (green), phalloidin (red) and nuclei with TO-PRO[®] 3 (blue); cell pseudopodia are highlighted with an asterisk. The panels on the right include magnified details in which white arrowheads indicate cell pseudopodia. Scale bar = 50 μm . Right: graph reporting the number of cell pseudopodia per cells as evaluated by counting. Statistics were obtained using the paired Student's t-test. (E) Left graph: quantification of MMRN2 staining normalized to CD31 in the whole cell monolayer respect to the migration front. Right graph: evaluation of MMRN2 staining in the cells of the migration front with respect to their pseudopodia. Data assessed with Volocity software. Statistics were obtained using the paired Student's t-test. (F) Representative images of whole mounted aortic rings embedded in collagen type I and stained with anti-MMRN2 (green) and anti-CD31 (red) antibodies. Nuclei were stained with TO-PRO[®] 3 (blue). White arrowheads highlight tips of the sprouting neovessels devoid of MMRN2 staining. Scale bar = 150 μm . Right graph: evaluation of the staining for MMRN2 normalized to that of CD31 in pre-existing vessels (PEV) compared to newly formed vessels (NFV). Statistics were obtained using the paired Student's t-test. The experiments were repeated at least three times and represent the mean \pm SD.

Fig. 2. Angiogenic stimuli decrease MMRN2 expression. (A) Levels of *MMRN2* mRNA following treatment with 30 ng/ml of VEGFA for the indicated time points. Statistics were obtained using the paired Student's t-test. (B) Levels of *MMRN2* mRNA following treatment with 30 ng/ml of FGF-2 for the indicated time points. Statistics were obtained using the paired Student's t-test. (C) Levels of *MMRN2* mRNA following treatment with the conditioned media from HT-29 cells at the indicated time points. Statistics were obtained using the paired Student's t-test. (D) Western blot analysis of *MMRN2* expression by HUVEC with 30 ng/ml of VEGFA at the indicated time points. β -actin was used for normalization and quantification. Statistics were obtained using the one-way ANOVA test. (E) Immunofluorescence analysis of *MMRN2* expression (green) in HUVEC with 30 ng/ml of VEGFA. The analyses were performed at the indicated time points and co-stained with phalloidin (red). Scale bar = 30 μ m. (F) Levels of *MMRN2* expression relative to β -actin as reported in (E). Statistics were obtained using the one-way ANOVA test. The experiments were repeated at least three times and data represent the mean \pm SD.

Fig. 3. MMRN2 is cleaved by MMP-2 and MMP-9. (A) Western blot analysis of MMP-2, MMP-9 and *MMRN2* expression following treatment of HUVEC with 30 ng/ml of VEGFA and in the presence of 20 μ M of the metalloproteinase inhibitor, GM6001. The top graph reports intensity of the *MMRN2* bands normalized to β -actin. (B,C) Coomassie blue stained SDS-PAGE analysis of *MMRN2* cleavage following treatment with MMP-2, MT-MMP1 (MT1) or PBS (control). Black arrowheads indicate full-length *MMRN2*, whereas red arrowheads indicate cleaved bands. (D) Western blot of recombinant, N-terminal FLAG- or C-terminal His-tagged *MMRN2* following treatment with MMP-9. Bands were detected with anti-His and anti-FLAG antibodies; black arrowheads denote full-length *MMRN2*, whereas red arrowheads indicate the proteolytically generated fragments. (E) Immunofluorescence of *MMRN2* (green) following treatment with 30 ng/ml of VEGFA or PBS (control) with MMP-2 or MMP-9 inhibitors, or vehicle (DMSO). Analyses were conducted at 3 and 6 hours following treatment. HUVEC were stained with phalloidin (red); scale bar = 30 μ m. (F) Quantification of *MMRN2* staining relative to β -actin as reported in (E).

Experiments were repeated at least three times, Statistics were obtained using the one-way ANOVA test and data represent the mean \pm SD.

Fig. 4. MMP-9 inhibition significantly decreases EC motility only in the presence of MMRN2.

(A,B) Representative Images of the scratch test assay (A) or immunofluorescence (B) performed on HUVEC transduced with control (siScr) or MMRN2 specific (siMMRN2) siRNA adenoviral constructs following treatment with vehicle (DMSO) or the MMP-9 inhibitor. The extent of cell migration is highlighted with dotted lines and arrows. Scale bar = 100 μ m. Graphs to the right of (A) report the distance covered by HUVEC and percentage of wound closure. Staining was carried out using the anti-MMRN2 antibody (green) and phalloidin (red). Nuclei were stained with TO-PRO[®] 3 (blue). Scale bar = 30 μ m. Higher magnifications are shown in the panels on the right of (B) and cell pseudopodia highlighted by white arrowheads. The graphs to the right (B) report the levels of MMRN2 expression relative to the number of detected nuclei. Number of migrating cells per field and number of pseudopodia per cell were assessed by counting. The experiments were repeated at least three times, and statistical values were obtained using the one-way ANOVA test. Data are reported as the mean \pm SD.

Fig. 5. Depletion of MMRN2 weakens the MMP-9 pro-migratory function. (A) Random motility of HUVEC transduced with control (siScr) or MMRN2 specific (siMMRN2) siRNA adenoviral constructs following treatment with recombinant MMP-9. (B) Quantification of speed, total, and euclid distance covered by HUVEC from the experiment in (A). Quantity of HUVEC per field following adhesion assays to MMRN2 with or without digestion in the presence of recombinant MMP-9 (MMRN2/MMP-9). Collagen type I was used as a control and effective cleavage of the molecule was verified by SDS-PAGE (right panel). Experiments were repeated at least three times, statistical values were obtained using the one-way ANOVA test, and reported as the mean \pm SD.

Fig. 6. MMRN2 expression is decreased in tumor-associated ECs. (A) Relative MMRN2 expression in ECs extracted from prostate (PTEC), breast (BTEC) and kidney (ECK). Expression in HUVEC and HDMEC were used as a reference. (B) Relative *MMRN2* expression in biopsies collected from normal and tumor tissues of various colorectal cancer patients. CD31 was used to normalize the vessels among the different biopsies (C) Representative images conducted on colorectal tumor samples using anti-MMP-9 (green) and anti-MMRN2 (red) antibodies. Nuclei were stained with TO-PRO[®] 3 (blue). Scale bar = 30 μ m. Experiments were repeated at least three times, statistical values were obtained using the one-way ANOVA test, and reported as the mean \pm SD.

Figure 1

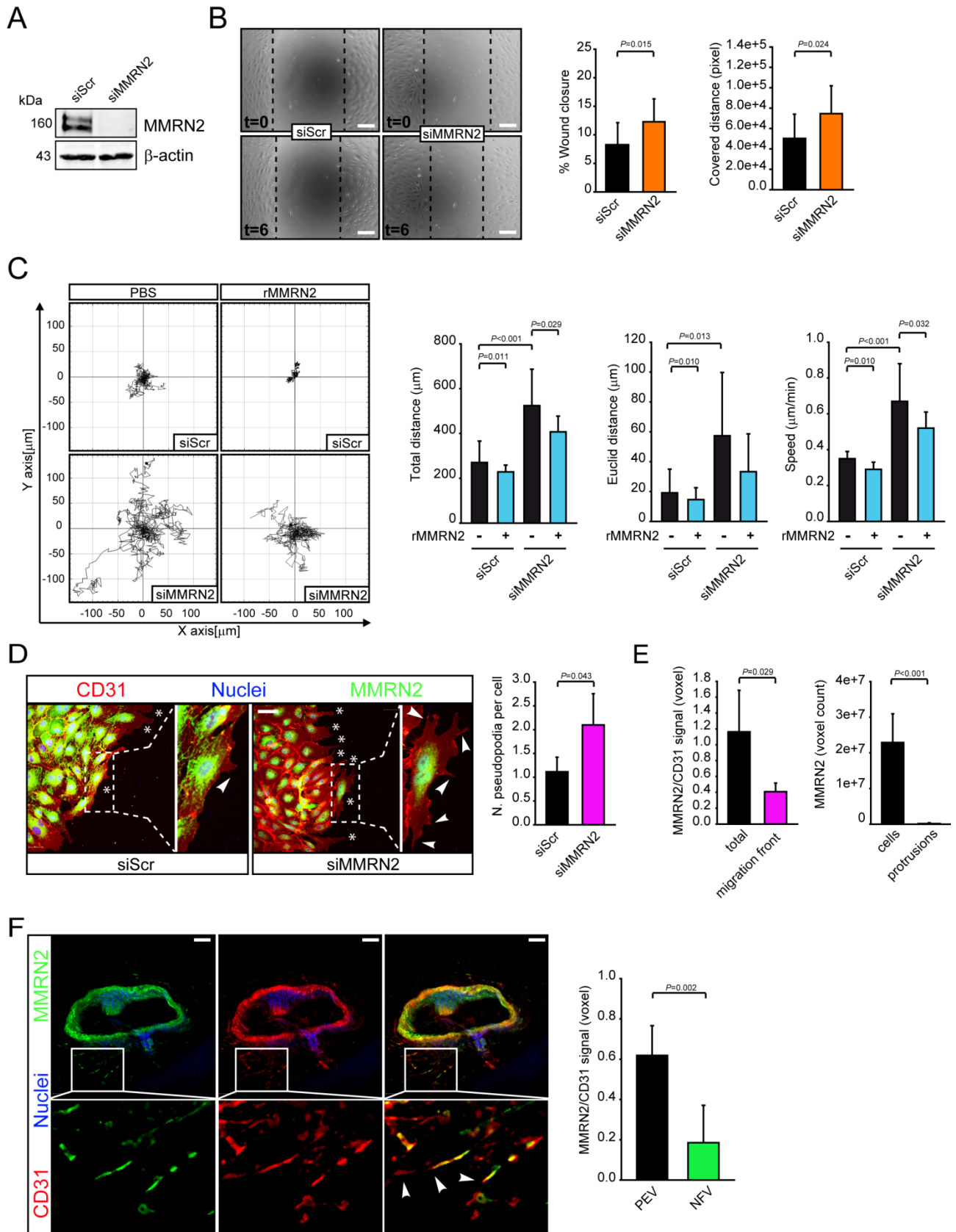


Figure 2

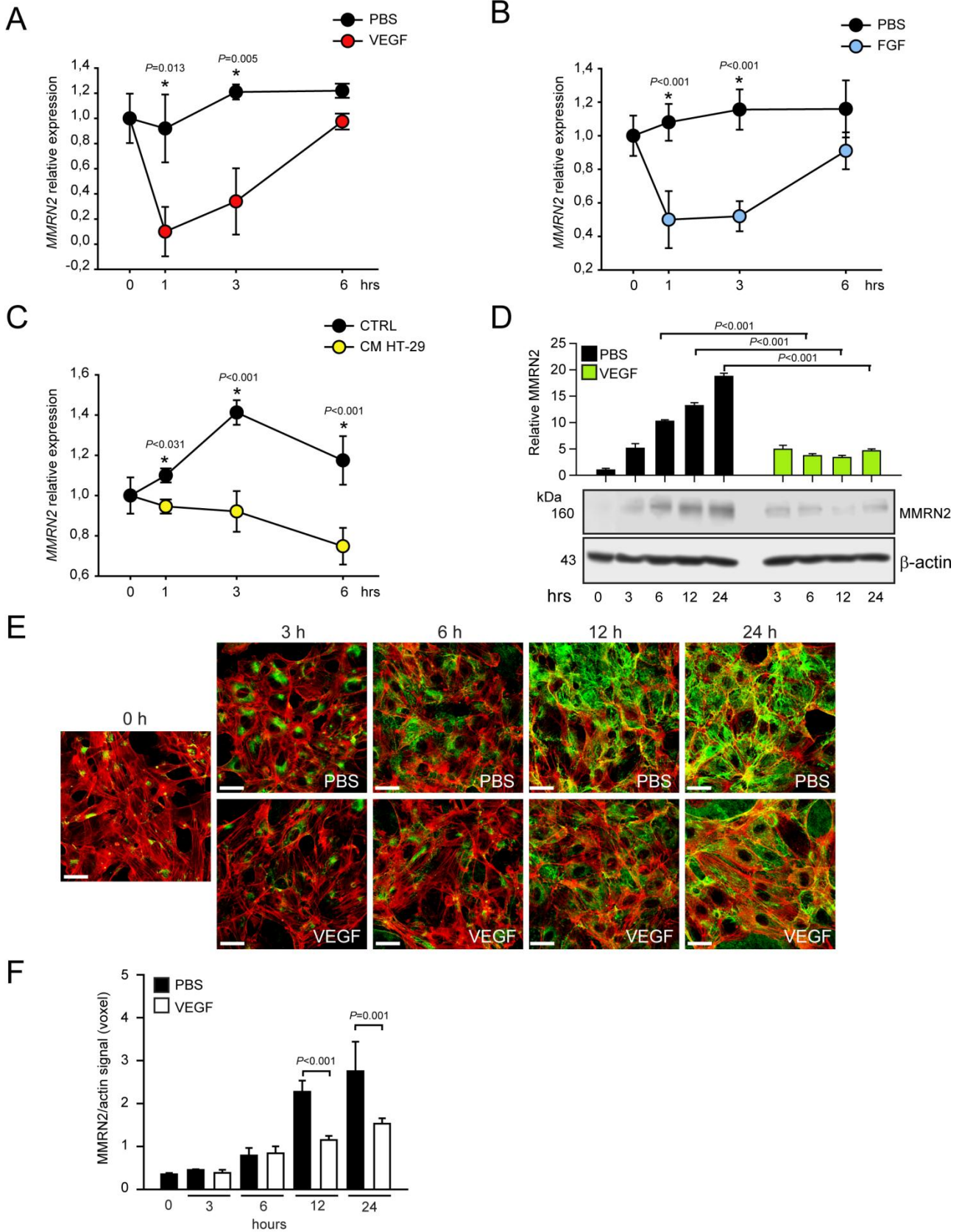


Figure 3

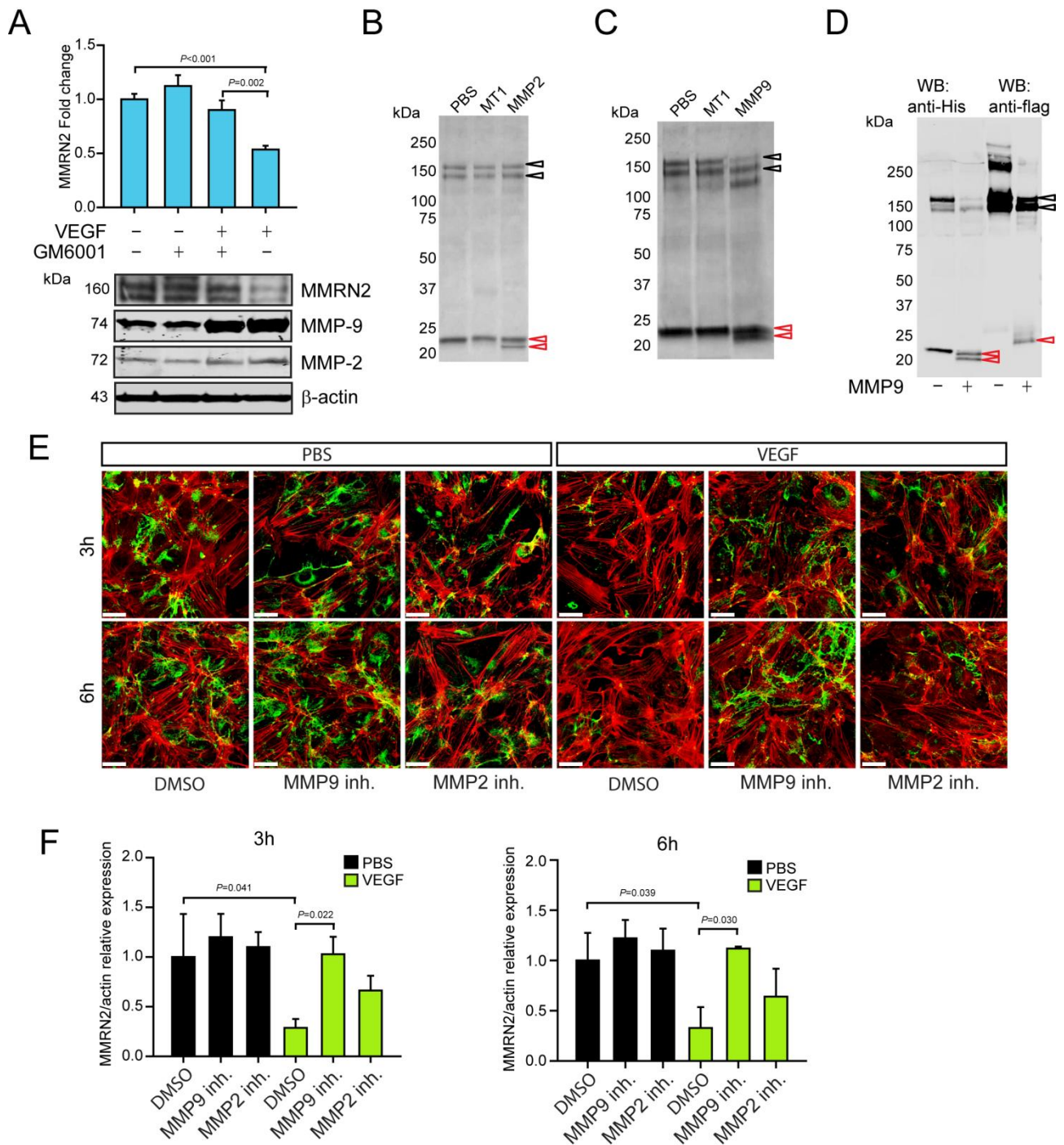
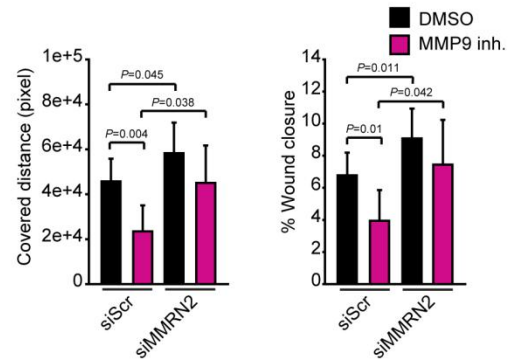
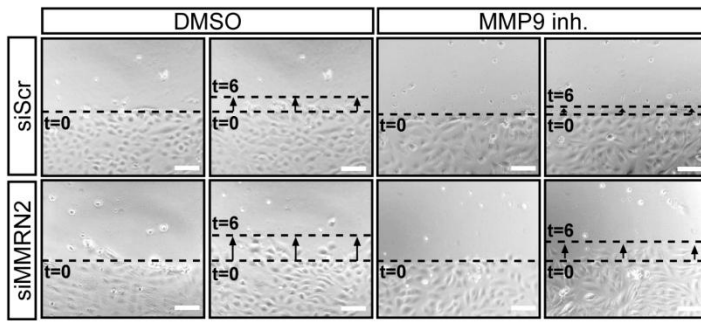


Figure 4

A



B

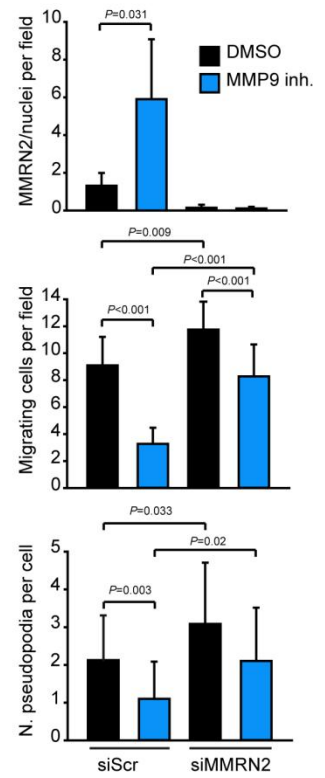
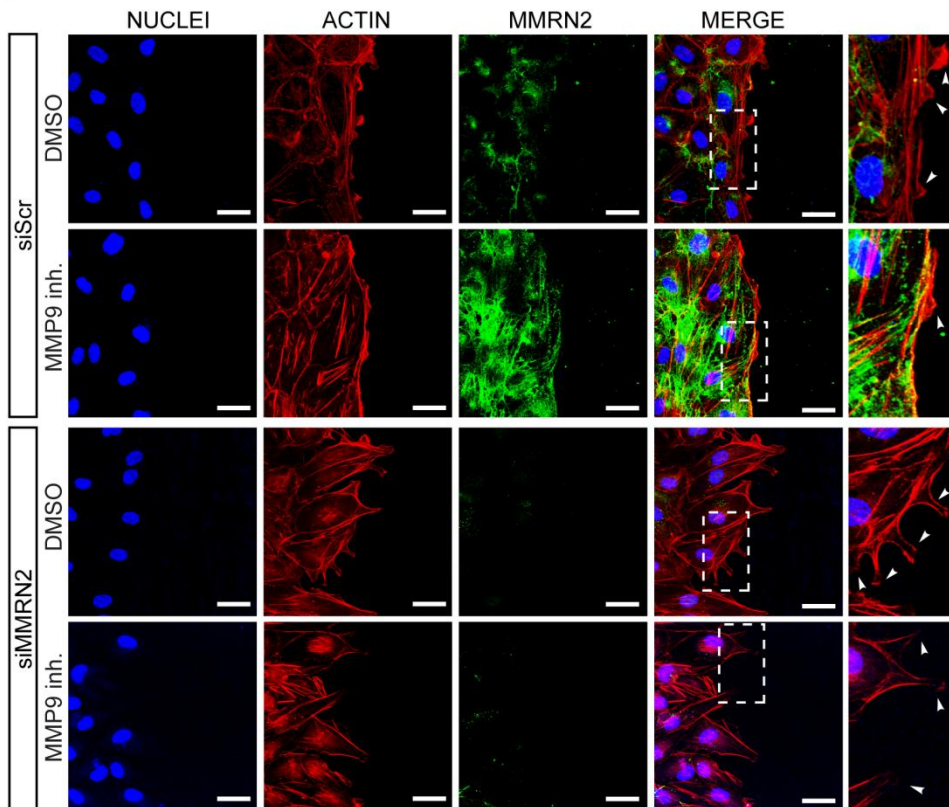


Figure 5

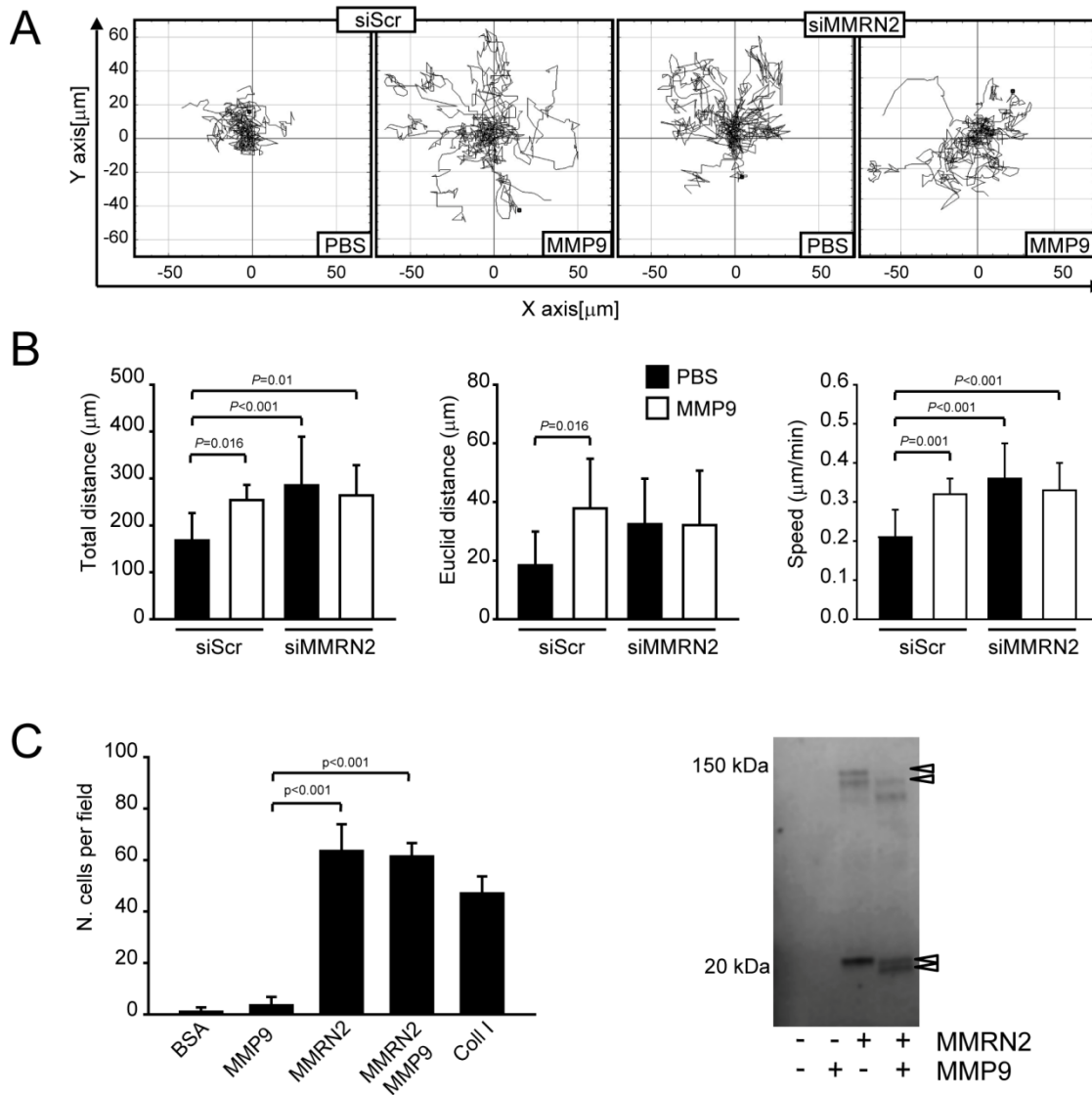
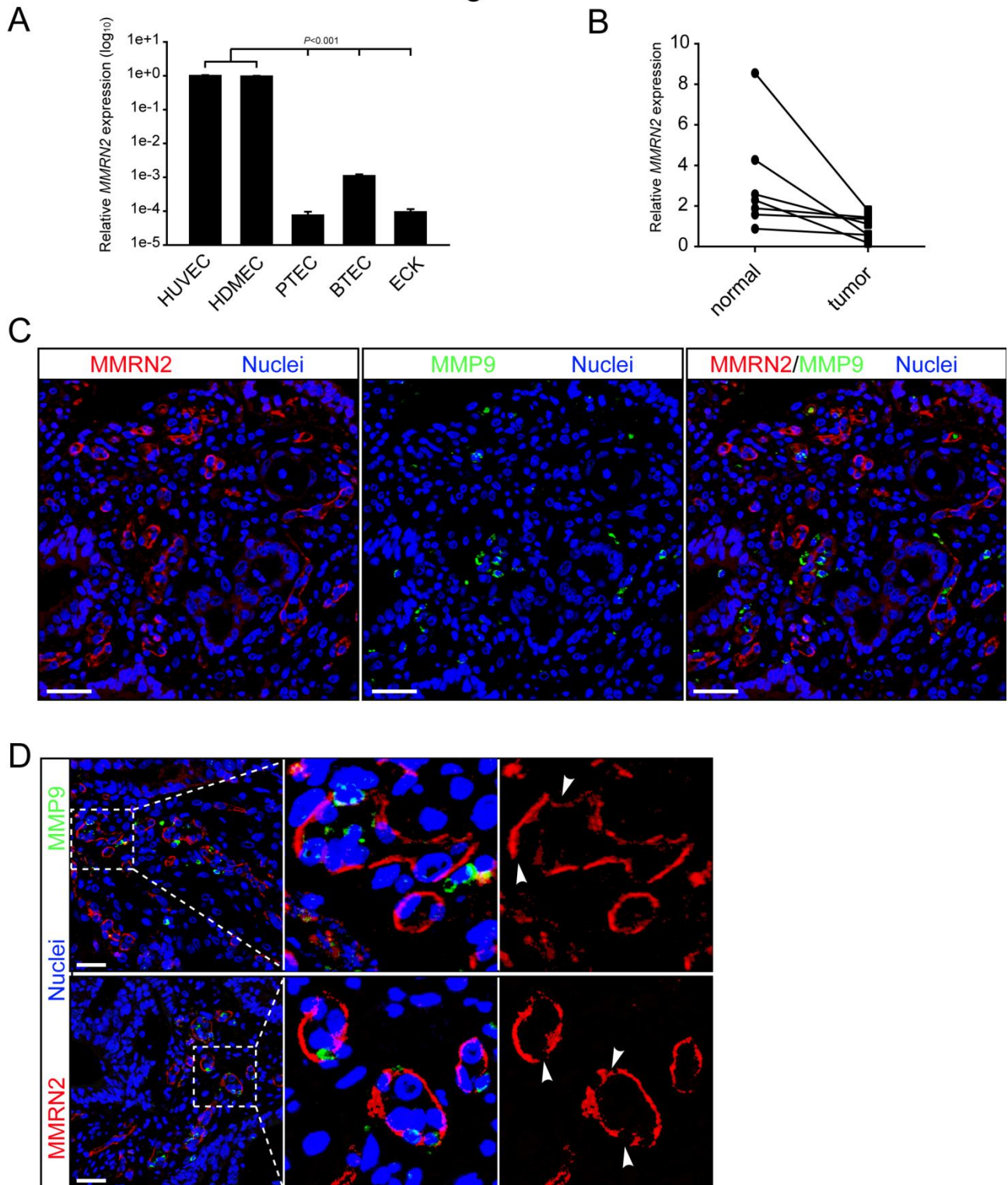


Figure 6



Highlights

- Sprouting angiogenesis is promoted by MMRN2 down-regulation and processing
- MMP-2 and MMP-9 target MMRN2 for degradation during angiogenesis
- MMRN2 expression is altered in tumor-associated angiogenesis
- Our data support a critical role for MMRN2 in regulating endothelial cell biology and angiogenesis